

KeyRe-ID: Keypoint-Guided Person Re-Identification using Part-Aware Representation in Videos

Jinseong Kim¹, Jeonghoon Song², Gyeongseon Baek², Byeongjoon Noh^{1,2*}

¹Department of AI and Big Data, Soonchunhyang University, 22 Soonchunhyang-ro, Asan, 31538, South Korea

²Department of Future Convergence Technology, Soonchunhyang University, 22 Soonchunhyang-ro, Asan, 31538, South Korea

Abstract

We propose **KeyRe-ID**, a keypoint-guided video-based person re-identification framework consisting of global and local branches that leverage human keypoints for enhanced spatiotemporal representation learning. The global branch captures holistic identity semantics through Transformer-based temporal aggregation, while the local branch dynamically segments body regions based on keypoints to generate fine-grained, part-aware features. Extensive experiments on MARS and iLIDS-VID benchmarks demonstrate state-of-the-art performance, achieving 91.73% mAP and 97.32% Rank-1 accuracy on MARS, and 96.00% Rank-1 and 100.0% Rank-5 accuracy on iLIDS-VID. Implementation details are available at: <https://github.com/JinSeong0115/KeyRe-ID>.

Introduction

Person Re-Identification (Re-ID) is the task of identifying and retrieving the same individual across non-overlapping camera views, and it has become a fundamental computer vision technology in a variety of real-world applications, including intelligent video surveillance, pedestrian tracking, autonomous driving, and smart city infrastructure (Ning et al. 2024; Xiao et al. 2024; Dou et al. 2023; Somers, Alahi, and Vleeschouwer 2024). Depending on the input modality, Re-ID can be categorized into image-based and video-based approaches. While image-based Re-ID extracts features from static still images, video-based Re-ID leverages temporally continuous frame sequences—referred to as tracklets, which are short video clips of a single person—to incorporate temporal dependencies and motion cues. This temporal modeling enables more robust performance in challenging environments characterized by occlusions, pose variations, and illumination changes (Wu et al. 2024; Huang et al. 2025; Zhang et al. 2024).

Early video-based Re-ID approaches primarily relied on CNNs to extract frame-level features, followed by post-hoc temporal aggregation methods (McLaughlin, Del Rincon, and Miller 2016; Zhou et al. 2017; Zhao et al. 2019; Yang et al. 2020). Recently, Transformer-based architectures have gained attention due to their ability to model long-range spatiotemporal dependencies via multi-head self-attention

mechanisms while preserving high-resolution feature representations—an advantage over conventional CNNs (Zhang et al. 2021; Alsehaim and Breckon 2022; Tang et al. 2022). Nonetheless, existing Transformer-based Re-ID frameworks commonly tokenize input frames using fixed-size patches or horizontal stripes, which limits their ability to adapt to fine-grained part-level motion and pose variations across frames.

To address these limitations, we propose **KeyRe-ID**, a keypoint-guided video person Re-ID framework designed to enhance part-level spatiotemporal representation learning. Instead of solely relying on patch divisions, our method incorporates keypoints—extracted from an external pose estimation model—to dynamically guide part segmentation on top of the patch-based tokenization. This dual-source approach enables the network to learn anatomically aligned part representations that more accurately capture body structure and motion patterns across frames. Each part-specific feature is temporally aggregated after undergoing clip-level perturbation to improve robustness under pose transitions.

In addition, a global representation is learned via a transformer-based global branch, following the architecture of VID-Trans-ReID (Alsehaim and Breckon 2022), enabling holistic clip-level identity modeling. The joint optimization of both global and keypoint-guided local branches enhances the model’s robustness to viewpoint changes, partial occlusions, and misalignment issues prevalent in real-world multi-camera environments. Extensive experiments on MARS and iLIDS-VID demonstrate that KeyRe-ID achieves state-of-the-art performance, validating its effectiveness in complex video-based Re-ID scenarios.

Extensive experiments conducted on two benchmark datasets, MARS (Zheng et al. 2016) and iLIDS-VID (Wang et al. 2014), validate the effectiveness of the proposed KeyRe-ID. The model achieves state-of-the-art (SOTA) performance, attaining a Rank-1 accuracy of 97.32% and mAP of 91.73% on MARS, and a Rank-5 accuracy of 100% on iLIDS-VID. To the best of our knowledge, this is the first Transformer-based video Re-ID framework that jointly addresses dynamic keypoint-guided part segmentation and temporal modeling, making a significant step toward practical and robust deployment of Re-ID systems in complex real-world environments.

*Corresponding author.

Related Works

Conventional video-based Re-ID approaches primarily rely on CNNs to extract frame-level visual features, followed by post-hoc temporal aggregation. However, these methods suffer from limited receptive fields and aggressive downsampling, which hinder their ability to capture spatiotemporal interactions effectively (Kim et al. 2025; He et al. 2021). To address this, Vision Transformer (ViT)-based architectures have been introduced, enabling direct modeling of long-range dependencies across frames (Liu et al. 2023). Models such as VID-Trans-ReID (Alsehaim and Breckon 2022), ST-Former (Zhang et al. 2021), and Dual-Path Transformer (Xia et al. 2024) leverage spatiotemporal attention over sampled clips to learn global representations (Wu et al. 2024). Yet, most of these methods rely on fixed patch-level tokenization, making them less effective at capturing fine-grained part-level motion and pose variations (Zhang et al. 2023).

To overcome this, part-aware methods have incorporated horizontal stripes or semantic parsing to model local body regions (Ren et al. 2022; Zhu et al. 2022; Kalayeh et al. 2018). However, these approaches depend on static partitioning or pre-defined parsing maps, limiting their adaptability to dynamic body movements and temporal misalignments (Wang et al. 2022; Wei et al. 2021). While some works utilize keypoints or parsing masks for part-level cues, they often lack temporal consistency and are not integrated within a unified framework (He et al. 2023; Dou et al. 2022; Zhou et al. 2020).

To address these gaps, our work builds on Transformer-based global modeling and introduces a unified framework that incorporates keypoint-guided dynamic part segmentation with temporal alignment. By jointly learning global and part-aware features, the proposed model enhances identification performance in complex, real-world scenarios.

Proposed Method

Preliminary

In this section, we describe the proposed **KeyRe-ID** framework for video-based person re-identification. As illustrated in Figure 1, the architecture comprises a shared spatiotemporal patch encoder followed by two specialized branches: a *global branch* that captures holistic clip-level features and a *local branch* that models fine-grained, part-aware cues guided by body keypoints. This design facilitates robust identity discrimination across varying poses and appearances. We begin by formalizing the input structure and intermediate representations that underpin our framework.

Given a video tracklet $V = \{I_1, I_2, \dots, I_N\}$ consisting of N RGB frames, we construct a temporally representative clip $\mathcal{C} = \{I_{s_1}, \dots, I_{s_T}\}$ by dividing the sequence into T equal segments and sampling one frame per segment. This promotes temporal diversity during training and continuity during inference.

Video feature representation

ViT backbone The ViT backbone serves as the primary feature extractor, encoding spatial semantics from each video frame while preserving the overall temporal structure.

Each input frame I_{s_t} is partitioned into overlapping patches of size $P \times P$ with stride s , yielding n patches per frame. Each patch is linearly projected into a D -dimensional embedding, and a learnable [CLS] token is prepended to each sequence to summarize global frame-level information.

For a sampled clip composed of T frames, the resulting token sequence is represented as:

$$\mathbf{Z} \in \mathbb{R}^{T \times (n+1) \times D} \quad (1)$$

where each token group consists of n patch tokens and one [CLS] token.

To encode spatial and camera-related priors, we apply a learnable spatiotemporal positional embedding **pos** and a camera-aware embedding **cam**, integrated as follows:

$$\tilde{\mathbf{Z}} = \mathbf{Z} + \lambda \cdot \mathbf{pos} + (1 - \lambda) \cdot \mathbf{cam} \quad (2)$$

This enriched sequence $\tilde{\mathbf{Z}}$ is then passed through the ViT backbone, producing spatiotemporal features, $\mathbf{F} \in \mathbb{R}^{T \times (n+1) \times D}$ which capture both local patch-level and global frame-level context. The output is decomposed into:

$$\mathbf{F}^{\text{cls}} \in \mathbb{R}^{T \times D}, \quad \mathbf{F}^{\text{patch}} \in \mathbb{R}^{T \times n \times D} \quad (3)$$

where \mathbf{F}^{cls} denotes the [CLS] token embeddings summarizing each frame, and $\mathbf{F}^{\text{patch}}$ represents the embeddings of all patch tokens.

This architectural design allows the global and local branches to specialize in complementary identity cues—clip-level semantics and part-level appearance—contributing to robust person re-identification under diverse motion and viewpoint conditions.

Keypoint-based part heatmap generation To improve part-aware representation learning in video-based person re-identification, this study utilizes keypoint heatmap information that reflects the human body structure. Prior video-based re-identification approaches have primarily relied on RGB visual cues, which often fail to robustly capture local identity-discriminative features under challenging conditions such as pose variations, occlusions, and background interference. To address these limitations, our framework incorporates structural spatial information derived from human joint locations. This design guides the model to attend to semantically meaningful body regions during feature learning, enabling the extraction of robust representations even under spatial misalignment and visual noise.

For each sampled frame I_{s_t} , human keypoints are extracted using a pretrained PifPaf pose estimator (Kreiss, Bertoni, and Alahi 2019), which returns J predefined joint coordinates. Each joint location is then transformed into a 2D Gaussian heatmap aligned with the input frame resolution:

$$\mathbf{h}_{s_t}^j \in \mathbb{R}^{H \times W}, \quad j = 1, \dots, J \quad (4)$$

where $\mathbf{h}_{s_t}^j$ represents the spatial likelihood distribution centered at the estimated joint position.

The extracted joints are then grouped into K semantically meaningful body parts, such as head, torso, arms, and legs, as summarized in Tab. 1. Each part k is associated with a set of joints denoted by \mathcal{J}_k , and the corresponding part-level

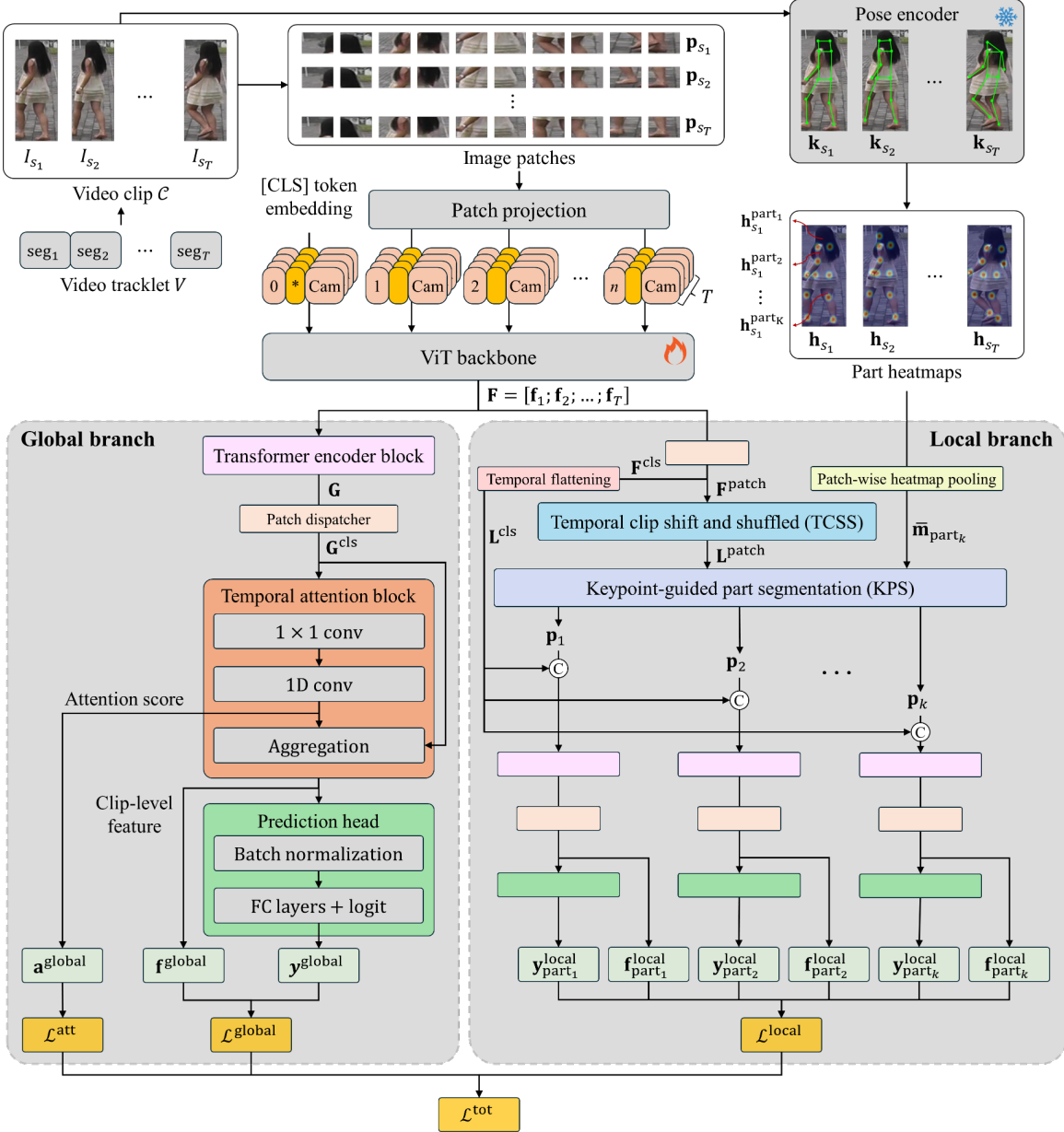


Figure 1: Overview of the training phase in the proposed **KeyRe-ID** framework. A video tracklet is segmented into temporal clips and processed by a shared *ViT backbone* to extract deep spatiotemporal features. The framework consists of two branches: the *Global branch* captures holistic identity cues by applying temporal attention over the extracted features, producing a clip-level representation. In parallel, the *Local branch* first perturbs patch-wise representations using the *TCSS module* to enhance temporal robustness. Subsequently, keypoint heatmaps are aggregated at the patch level and used in the *KPS module* to generate body-part-specific features. Both branches are independently supervised by dedicated loss functions, and their outputs are jointly optimized through a composite objective to improve identity discrimination across pose and appearance variations.

heatmap is obtained by averaging the heatmaps of its constituent joints:

$$\mathbf{h}_{s_t}^{\text{part}_k} = \frac{1}{|\mathcal{J}_k|} \sum_{j \in \mathcal{J}_k} \mathbf{h}_{s_t}^j, \quad k = 1, \dots, K \quad (5)$$

These part-specific heatmaps preserve the structural spatial distribution of the person in each frame and serve as aux-

iliary information for local feature learning. In subsequent modules, they are aligned with visual patch tokens to facilitate region-level attention, thereby improving the discriminative power of local features under various spatial perturbations.

Part	Joints
Head	Eyes (left/right), ears (left/right), nose
Torso	Shoulders (left/right), hip (left/right)
Arms (left/right)	Elbows and wrists (left/right)
Legs (left/right)	Knees and ankles (left/right)

Table 1: Definition of the six body parts used in our framework, based on grouped keypoint joints.

Global branch

The primary role of the global branch is to predict the identity of the person depicted in the input video clip, denoted as *Global_ID*. To this end, it produces a discriminative clip-level representation by temporally aggregating frame-wise semantic features. Instead of explicitly modeling long-range temporal dependencies, this branch focuses on adaptive temporal integration using attention mechanisms. The overall design follows the principles of *VID-Trans-ReID* model (Alsehaim and Breckon 2022), while incorporating a transformer encoder for enhanced contextual reasoning.

Given the frame-wise feature sequence $\mathbf{F} \in \mathbb{R}^{T \times (n+1) \times D}$ generated by the ViT backbone, we first pass it through a dedicated *transformer encoder block* \mathcal{T} , which enables spatiotemporal feature refinement via multi-head self-attention across all tokens:

$$\mathbf{G} = \mathcal{T}(\mathbf{F}) \in \mathbb{R}^{T \times (n+1) \times D} \quad (6)$$

To prepare the input for *temporal attention block*, we extract the set of [CLS] tokens from \mathbf{G} , denoted as:

$$\mathbf{G}^{\text{cls}} = \{\mathbf{g}_1^{\text{cls}}, \dots, \mathbf{g}_T^{\text{cls}}\} \in \mathbb{R}^{T \times D} \quad (7)$$

These tokens compactly summarize frame-level semantics and serve as the foundation for frame-wise attention computation and subsequent clip-level representation learning. At this stage, a *patch dispatcher* is used to decouple the [CLS] tokens from the remaining patch tokens. This separation enables the model to process global clip representations and local patch-wise representations independently in the subsequent branches.

Temporal attention and aggregation To identify temporally salient frames that contribute most to identity discrimination, we apply a temporal attention module composed of a 2D convolution followed by a 1D temporal convolution applied to the frame-wise [CLS] features. This operation produces a raw attention score vector $\mathbf{a}^{\text{global}} \in \mathbb{R}^T$. The scores are normalized using a softmax function to obtain temporal attention weights $\alpha = \{\alpha_1, \dots, \alpha_T\}$, which quantify the relative importance of each frame within the video clip.

Using these attention weights, we compute the clip-level representation as a weighted sum of the [CLS] tokens:

$$\mathbf{f}^{\text{global}} = \sum_{t=1}^T \alpha_t \cdot \mathbf{g}_t^{\text{cls}} \quad (8)$$

Prediction head The aggregated feature $\mathbf{f}^{\text{global}}$ is passed through a *prediction head* consisting of batch normalization

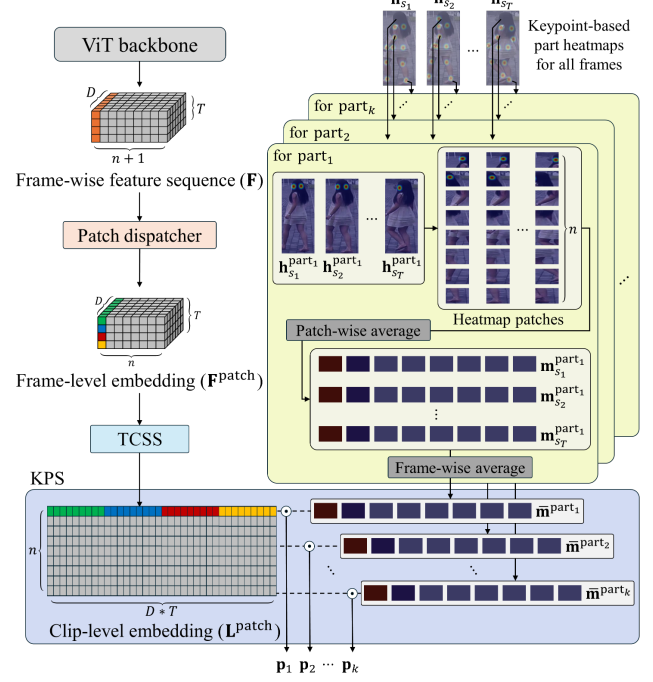


Figure 2: In the *KPS module*, the operation to obtain part-aware spatio-temporal features involves averaging the part heatmaps across patch and frame dimensions to produce part-specific embeddings, which are then combined with the clip-level features from the *TCSS module* through element-wise multiplication.

and fully connected layers, yielding the final global embedding $\mathbf{y}^{\text{global}}$. This embedding is directly used to predict the clip-level identity label *Global_ID*, which corresponds to the person represented in the video.

All outputs from this branch—including the attention scores $\mathbf{a}^{\text{global}}$, the clip-level representation $\mathbf{f}^{\text{global}}$, and the final global embedding $\mathbf{y}^{\text{global}}$ —are jointly optimized via a composite loss function. This function incorporates classification loss, triplet loss, and an attention regularization loss. Further implementation details are provided in the **Model optimization** section.

Local branch

The local branch extracts fine-grained and part-aware discriminative features by integrating keypoint-guided spatial cues into the video-based Re-ID process. Unlike the global branch that captures holistic clip-level semantics, the local branch enhances robustness against occlusions and pose variations through temporal perturbations and body part-level aggregation.

Temporal clip shift and shuffle (TCSS) Patch-level features in video-based Re-ID can suffer from overfitting to fixed temporal patterns or frame-specific biases, especially under challenging conditions like occlusion or abrupt motion. To mitigate this, we adopt the *TCSS module*, which perturbs the temporal structure of patch tokens, promoting more robust feature learning.

Instead of relying on strict sequential order, *TCSS module* applies a circular temporal shift to each patch-level feature across frames, followed by a patch-wise shuffling operation (Zhang et al. 2018). This introduces temporal diversity, reduces reliance on exact frame order, and encourages richer feature representations. Our TCSS extends the original *VID-Trans-ReID* design (Alsehaim and Breckon 2022) by subsequently incorporating keypoint-guided part information.

Patch-wise heatmap pooling To guide patch-level representation learning, we construct part-specific patch importance vectors from detected human keypoints. The keypoints of each frame are grouped into K semantically meaningful body parts, and part heatmaps are obtained by averaging the corresponding joint heatmaps. These part heatmaps are downsampled via average pooling to match the patch grid, producing per-frame part-to-patch importance vectors.

For each part k , we average these vectors over T frames to obtain a clip-level importance vector $\bar{\mathbf{m}}_{\text{part}_k}$. This vector semantically aligns body parts with patch tokens, facilitating robust feature encoding under pose and motion variations.

Keypoint-guided part segmentation (KPS) As one of the core contributions of this study, the *KPS module* addresses the limitations of conventional methods that rely solely on static patch structures, constructing semantically aligned local features by integrating keypoint-guided part importance with temporally structured patch representation.

As shown in Figure 2, *KPS module* utilizes temporally ordered patch features $\mathbf{L}^{\text{patch}} \in \mathbb{R}^{n \times (T \cdot D)}$, obtained through TCSS, and the clip-level part-specific importance vectors $\bar{\mathbf{m}}^{\text{part}_k}$. These vectors encode patch relevance per body part, serving as soft attention maps.

To obtain part-aware spatio-temporal features, we perform element-wise multiplication: $\mathbf{p}_k = \mathbf{L}^{\text{patch}} \odot \bar{\mathbf{m}}^{\text{part}_k}$. The result \mathbf{p}_k is concatenated with the [CLS] token embedding \mathbf{L}^{cls} , which is the temporally flattened vector of \mathbf{F}^{cls} , and passed through a transformer encoder for context enrichment.

The output sequence from the transformer encoder is subsequently passed through a patch dispatcher; the [CLS]-associated token is used as the part-level identity feature $\mathbf{f}_{\text{part}_k}^{\text{local}}$, which is then passed through the *prediction head* to produce the part-level identity feature $\mathbf{y}_{\text{part}_k}^{\text{local}}$, following the same design as in the *global branch*. The overall local supervision is applied through the local loss $\mathcal{L}^{\text{local}}$, which is jointly optimized with the global loss $\mathcal{L}^{\text{global}}$ as part of the total training objective.

Model optimization

The proposed KeyRe-ID framework is trained in an end-to-end manner through two phases: training and inference.

Training phase During training, the model is optimized with multi-branch loss strategy that jointly supervises global and part-aware (local) representations. The overall loss integrates global and local branch objectives as follows:

$$\mathcal{L}^{\text{tot}} = \alpha \cdot \mathcal{L}^{\text{global}} + (1 - \alpha) \cdot \mathcal{L}^{\text{local}} \quad (9)$$

where α_g and α_l are trade-off parameters. This formulation facilitates complementary learning between coarse-grained and fine-grained features.

The *global branch* loss $\mathcal{L}^{\text{global}}$ supervises a clip-level embedding that aggregates temporal identity information. It combines cross-entropy identity classification loss with label smoothing (Szegedy et al. 2016), triplet loss for inter-class margin maximization (Hermans, Beyer, and Leibe 2017), center loss for intra-class compactness (Wen et al. 2016), and attention regularization to penalize reliance on potentially occluded frames (Pathak, Eshratifar, and Gormish 2020). Formally, it is defined as:

$$\mathcal{L}^{\text{global}} = \mathcal{L}^{\text{ID}} + \mathcal{L}^{\text{triplet}} + \beta \cdot \mathcal{L}^{\text{center}} + \mathcal{L}^{\text{attn}} \quad (10)$$

where λ_{center} is a weighting coefficients. The classification loss \mathcal{L}^{ID} is computed from the predicted identity $\mathbf{y}^{\text{global}}$, while the triplet and center losses are applied to the embedding $\mathbf{f}^{\text{global}}$.

The *local branch* loss $\mathcal{L}^{\text{local}}$ supervises part-specific embeddings, independently optimized for each body part. Similar to the *global branch*, it includes identity classification, triplet loss, and center loss for each part k :

$$\mathcal{L}^{\text{local}} = \frac{1}{K} \sum_{k=1}^K \left(\mathcal{L}_k^{\text{ID}} + \mathcal{L}_k^{\text{triplet}} + \beta \cdot \mathcal{L}_k^{\text{center}} \right) \quad (11)$$

This enables fine-grained supervision of local features, enhancing robustness to occlusions and pose variations. All model components are jointly optimized through back-propagation.

Inference phase During inference, the KeyRe-ID model identifies individuals by comparing the extracted features of a query tracklet with those in a gallery, which stores concatenated global and part-aware embeddings of previously observed persons, typically collected from multi-camera environments. For each query, the model extracts a global embedding and multiple part-specific embeddings, corresponding to predefined body regions. These features are concatenated to form the final descriptor, which is compared against all gallery entries using Euclidean distance.

Validation

Experimental setup

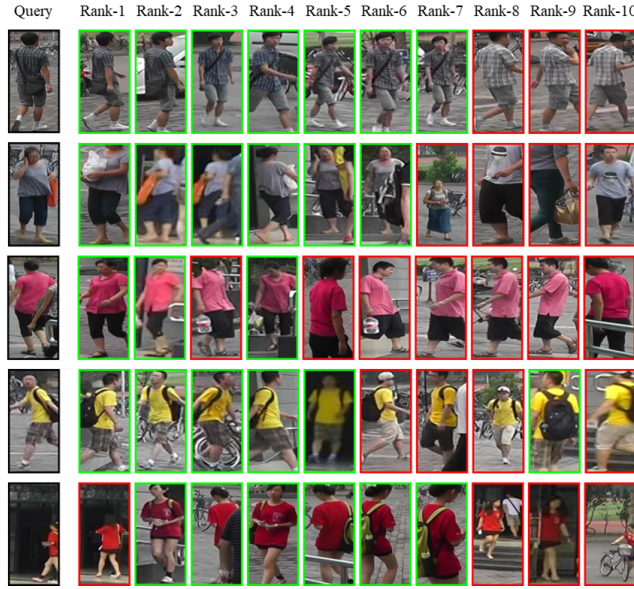
Datasets We evaluate our method on two widely used video-based person Re-ID benchmarks:

- **MARS** (Zheng et al. 2016): is the largest benchmark in this domain, comprising 1,261 identities and 20,715 tracklets captured from 6 cameras.
- **iLIDS-VID** (Li, Zhu, and Gong 2018): contains 300 identities and 600 tracklets recorded across 2 cameras, offering more challenging variations in viewpoint and occlusion under limited data.

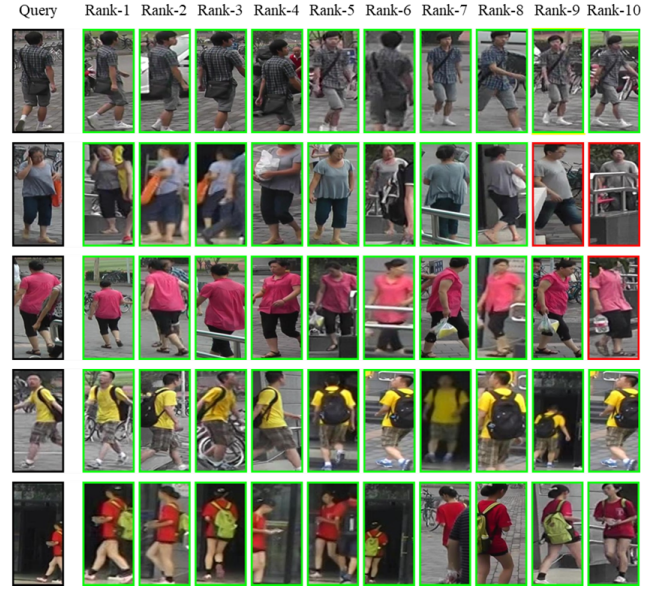
Evaluation metrics On MARS, we report Average Precision (mAP) and Rank-1 accuracy due to its multi-shot structure. For iLIDS-VID, we report Rank-1 and Rank-5 accuracy. mAP measures average retrieval precision across ranks, while Rank-k indicates the probability of finding a correct match within the top-k retrieved results.

Method	MARS		iLIDS-VID		Method	MARS		iLIDS-VID	
	mAP	Rank-1	Rank-1	Rank-5		mAP	Rank-1	Rank-1	Rank-5
STMP (Liu et al. 2019)	72.7	84.4	84.3	96.8	CTL (Liu et al. 2021a)	86.7	91.4	89.7	97.0
M3D (Li, Zhang, and Huang 2020)	74.1	84.4	74.0	94.3	PSTA (Wang et al. 2021)	85.8	91.5	91.5	98.1
GLTR (Li et al. 2019)	78.5	87.0	86.0	98.0	KSTL (Guo and Wang 2023)	86.3	91.5	93.4	–
RethinkingTF (Jiang et al. 2020)	85.2	87.1	87.7	–	CRF (Bai, Chang, and Ma 2024)	87.4	91.5	93.4	–
Co-Aware (Wu et al. 2021)	84.1	88.2	85.8	–	TCViT (Wu et al. 2024)	87.6	91.7	94.3	99.3
VRSTC (Hou et al. 2019)	82.3	88.5	83.4	95.5	KMPN (MGH) (Chen et al. 2022)	86.6	92.0	–	–
MG-RAFA (Zhang et al. 2020)	85.6	88.8	88.6	98.0	PSFormer (Zhu et al. 2025)	88.2	92.1	93.7	99.5
MGH (Yan et al. 2020)	85.8	90.0	85.6	97.1	DCCT (Liu et al. 2023)	87.5	92.3	91.7	98.6
SSN3D (Jiang et al. 2021)	86.2	90.1	–	–	TF-CLIP (Yu et al. 2024)	89.4	93.0	94.5	99.1
PiT (Zang, Li, and Gao 2022)	86.8	90.2	92.1	98.9	CLIMB-ReID (Yu et al. 2025)	89.7	93.3	96.7	99.9
GRL (Liu et al. 2021b)	84.8	91.0	90.4	98.3	STFE (Yang et al. 2024)	91.5	95.5	–	–
SINet (Bai et al. 2022)	86.2	91.0	92.5	–	VID-Trans-ReID (Alsehaim and Breckon 2022)	90.2	96.36	94.67	–
DSANet (Kim, Cho, and Lee 2023)	86.6	91.1	85.1	75.5	KeyRe-ID (Ours)	91.73	97.32	96.0	100.0

Table 2: Comparison of video-based person re-identification methods on the MARS and iLIDS-VID datasets, reporting mAP and Rank-1 for MARS, and Rank-1 and Rank-5 for iLIDS-VID (sorted by MARS Rank-1 ascending).



(a) Retrieval results of *VID-Trans-ReID*



(b) Retrieval results of *KeyRe-ID*

Figure 3: Comparison of the results of top-10 retrieval results for two video-based Re-ID models on the MARS dataset. For each query image (leftmost), the top-10 ranked gallery images are shown from left to right. Green boxes denote correct matches, and red boxes denote incorrect ones.

Baselines We compare our method with a wide range of Re-ID models. Among them, *VID-Trans-ReID* (Alsehaim and Breckon 2022), which achieves the highest Rank-1 accuracy on the MARS dataset, is selected as our primary comparison target.

Implementation details Input frames are resized to 256×128 , and the model is trained for 120 epochs using SGD (learning rate: 0.008, batch size: 32, momentum: 0.9)) with cosine scheduling and 5 warm-up epochs. Each training sample is a randomly augmented 4-frame clip with horizontal flipping and random erasing. We adopt a 12-layer ViT backbone with number of patches ($P = 16$, stride $s = 16$, dimension $D = 768$) pretrained on ImageNet-21K. TCSS shift size is set to 5, and KPS uses 6 parts from 17 keypoints. Loss weights are $\alpha = 0.75$ and $\beta = 0.0005$.

Main results

Tab. 2 presents the results of the proposed KeyRe-ID method compared to other methods on MARS and iLIDS-VID datasets. On MARS, the proposed KeyRe-ID achieves SOTA performance with an mAP of 91.73% and Rank-1 accuracy of 97.32%, surpassing *VID-Trans-ReID* model (mAP 90.25%, Rank-1 96.36%). On iLIDS-VID, our method attains Rank-1 accuracy of 96.00% and perfect Rank-5 accuracy (100.0%), surpassing the *CLIMB-ReID*'s Rank-5 (99.9%) accuracy, and closely matching its Rank-1 (96.7%). These results confirm that the proposed method effectively combines transformer-based global modeling with keypoint-guided part-aware learning via TCSS and KPS, leading to improved spatiotemporal identity discrimination and setting new benchmarks for video person Re-ID.

MARS						
Global branch	Local branch	TCSS	KPS	mAP	Rank-1	
✓	✓	✗	✓	90.73	96.91	
✓	✓	✓	✗	90.25	96.36	
✓	✗	✗	✗	88.35	95.50	
✗	✓	✓	✓	85.74	95.88	
✓	✓	✓	✓	91.73	97.32	
iLIDS-VID						
Global branch	Local branch	TCSS	KPS	Rank-1	Rank-5	
✓	✓	✗	✓	94.00	100.00	
✓	✓	✓	✗	94.67	99.50	
✓	✗	✗	✗	89.33	98.67	
✗	✓	✓	✓	94.67	97.33	
✓	✓	✓	✓	96.00	100.00	

Table 3: Ablation study results under different architectural configurations on the MARS and iLIDS-VID datasets. The check mark (✓) indicates that the corresponding component is included, while the cross (✗) denotes its exclusion.

Ranking list Figure 3 shows qualitative top-10 retrieval results on the MARS dataset. VID-Trans-ReID frequently yields incorrect matches (red boxes) due to the inherent limitations of stripe-based segmentation, especially under challenging conditions involving pose variations and similar local appearances across different individuals. Conversely, KeyRe-ID, benefiting from KPS-based semantic segmentation, consistently delivers accurate top-ranking matches (green boxes). This clearly illustrates the robustness and improved discriminative capability of KeyRe-ID, attributable to anatomically-aligned, part-aware feature representations.

Attention map comparison We provide qualitative comparisons between VID-Trans-ReID and KeyRe-ID through attention map visualizations (Figure 4). VID-Trans-ReID, which relies on fixed stripe-based segmentation, produces rigid and narrowly localized activations, limiting its adaptability to diverse human poses. In contrast, KeyRe-ID integrates keypoint-guided spatial priors to dynamically align attention maps with semantically meaningful body parts. This structured attention not only enables broader and more balanced spatial coverage, but also enhances interpretability by clearly highlighting informative regions of each body part. As a result, KeyRe-ID effectively captures fine-grained identity cues, contributing to improved retrieval accuracy and robustness under varied visual conditions.

Ablation studies

To assess the contribution of each component in the proposed framework, we conduct comprehensive ablation experiments, as shown in Tab. 3. Removing the TCSS module results in a noticeable decline in performance, indicating its importance in enhancing temporal robustness against frame-level misalignment and motion perturbation. Excluding the KPS module reduces the mAP by 1.48% on the MARS dataset, highlighting the role of keypoint-guided spatial guidance in improving part-aware feature discrimina-

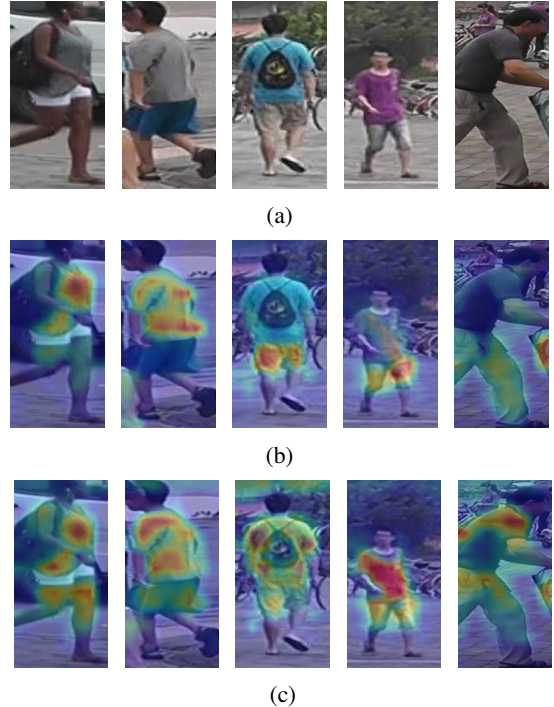


Figure 4: Attention maps on (a) input query images: (b) by VID-Trans-ReID that exhibits scattered and context-insensitive focus across the body, and (c) by KeyRe-ID that shows more consistent and semantically meaningful activations on identity-discriminative regions.

tion. The removal of the local branch leads to a significant performance drop, especially on MARS, underscoring its critical role in capturing fine-grained identity cues. Similarly, removing the global branch causes a marked degradation in overall accuracy (MARS mAP: 85.74%, Rank-1: 95.88%), demonstrating the necessity of holistic feature modeling. Collectively, the full KeyRe-ID model, incorporating all proposed components, achieves the highest performance across datasets, validating the complementary strengths and synergistic benefits of joint global and local representation learning.

Conclusion

In this paper, we proposed KeyRe-ID, a novel video-based person re-identification framework that leverages human keypoints to guide part-level representation learning. Built upon ViT backbone, KeyRe-ID integrates global and local branches, with the global branch aggregating clip-level semantic features via temporal attention, and the local branch employing KPS to construct fine-grained, part-aware features robust to pose variations. Extensive experiments on two widely-used benchmarks, MARS and iLIDS-VID, demonstrated the effectiveness of our method, achieving SOTA performance with Rank-1 accuracy of 97.32% and mAP of 91.73% on MARS, as well as Rank-1 accuracy of 96.00% and Rank-5 accuracy of about 100.0% on iLIDS-VID. Qualitative analysis confirmed that the KPS module

enhances feature alignment with human anatomical structures, thereby improving the accuracy of top-ranked retrieval results. Ablation studies validated the contributions of both TCSS and KPS modules in boosting overall performance.

References

Alsehaim, A.; and Breckon, T. 2022. VID-Trans-ReID: Enhanced Video Transformers for Person Re-identification. In *Proc. British Machine Vision Conference*. BMVA.

Bai, S.; Chang, H.; and Ma, B. 2024. Incorporating texture and silhouette for video-based person re-identification. *Pattern Recognition*, 156: 110759.

Bai, S.; Ma, B.; Chang, H.; Huang, R.; and Chen, X. 2022. Salient-to-broad transition for video person re-identification. In *Proceedings of the IEEE/CVF conference on computer vision and pattern recognition*, 7339–7348.

Chen, D.; Doering, A.; Zhang, S.; Yang, J.; Gall, J.; and Schiele, B. 2022. Keypoint message passing for video-based person re-identification. In *Proceedings of the AAAI Conference on Artificial Intelligence*, volume 36, 239–247.

Dou, S.; Zhao, C.; Jiang, X.; Zhang, S.; Zheng, W.-S.; and Zuo, W. 2022. Human co-parsing guided alignment for occluded person re-identification. *IEEE Transactions on Image Processing*, 32: 458–470.

Dou, Z.; Wang, Z.; Li, Y.; and Wang, S. 2023. Identity-seeking self-supervised representation learning for generalizable person re-identification. In *Proceedings of the IEEE/CVF international conference on computer vision*, 15847–15858.

Guo, W.; and Wang, H. 2023. Key Parts Spatio-Temporal Learning for Video Person Re-identification. In *Proceedings of the 5th ACM International Conference on Multimedia in Asia*, 1–6.

He, S.; Chen, W.; Wang, K.; Luo, H.; Wang, F.; Jiang, W.; and Ding, H. 2023. Region generation and assessment network for occluded person re-identification. *IEEE transactions on information forensics and security*, 19: 120–132.

He, S.; Luo, H.; Wang, P.; Wang, F.; Li, H.; and Jiang, W. 2021. Transreid: Transformer-based object re-identification. In *Proceedings of the IEEE/CVF international conference on computer vision*, 15013–15022.

Hermans, A.; Beyer, L.; and Leibe, B. 2017. In defense of the triplet loss for person re-identification. *arXiv preprint arXiv:1703.07737*.

Hou, R.; Ma, B.; Chang, H.; Gu, X.; Shan, S.; and Chen, X. 2019. Vrstc: Occlusion-free video person re-identification. In *Proceedings of the IEEE/CVF conference on computer vision and pattern recognition*, 7183–7192.

Huang, S.; Prabhakar, R.; Guo, Y.; Chellappa, R.; and Peng, C. 2025. VILLS: Video-Image Learning to Learn Semantics for Person Re-Identification. In *2025 IEEE/CVF Winter Conference on Applications of Computer Vision (WACV)*, 5969–5979. IEEE.

Jiang, X.; Gong, Y.; Guo, X.; Yang, Q.; Huang, F.; Zheng, W.-S.; Zheng, F.; and Sun, X. 2020. Rethinking temporal fusion for video-based person re-identification on semantic and time aspect. In *Proceedings of the AAAI Conference on Artificial Intelligence*, volume 34, 11133–11140.

Jiang, X.; Qiao, Y.; Yan, J.; Li, Q.; Zheng, W.; and Chen, D. 2021. SSN3D: Self-separated network to align parts for 3D convolution in video person re-identification. In *Proceedings of the AAAI conference on artificial intelligence*, volume 35, 1691–1699.

Kalayeh, M. M.; Basaran, E.; Gökmén, M.; Kamasak, M. E.; and Shah, M. 2018. Human semantic parsing for person re-identification. In *Proceedings of the IEEE conference on computer vision and pattern recognition*, 1062–1071.

Kim, M.; Cho, M.; Lee, H.; and Lee, S. 2025. Spatio-temporal Feature-level Augmentation Vision Transformer for video-based person re-identification. *Pattern Recognition*, 111813.

Kim, M.; Cho, M.; and Lee, S. 2023. Feature disentanglement learning with switching and aggregation for video-based person re-identification. In *Proceedings of the IEEE/CVF Winter Conference on Applications of Computer Vision*, 1603–1612.

Kreiss, S.; Bertoni, L.; and Alahi, A. 2019. Pifpaf: Composite fields for human pose estimation. In *Proceedings of the IEEE/CVF conference on computer vision and pattern recognition*, 11977–11986.

Li, J.; Wang, J.; Tian, Q.; Gao, W.; and Zhang, S. 2019. Global-local temporal representations for video person re-identification. In *Proceedings of the IEEE/CVF international conference on computer vision*, 3958–3967.

Li, J.; Zhang, S.; and Huang, T. 2020. Multi-scale temporal cues learning for video person re-identification. *IEEE Transactions on Image Processing*, 29: 4461–4473.

Li, M.; Zhu, X.; and Gong, S. 2018. Unsupervised Person Re-identification by Deep Learning Tracklet Association. In *Proceedings of the European Conference on Computer Vision (ECCV)*.

Liu, J.; Sun, C.; Xu, X.; Xu, B.; and Yu, S. 2019. A spatial and temporal features mixture model with body parts for video-based person re-identification. *Applied Intelligence*, 49: 3436–3446.

Liu, J.; Zha, Z.-J.; Wu, W.; Zheng, K.; and Sun, Q. 2021a. Spatial-temporal correlation and topology learning for person re-identification in videos. In *Proceedings of the IEEE/CVF conference on computer vision and pattern recognition*, 4370–4379.

Liu, X.; Yu, C.; Zhang, P.; and Lu, H. 2023. Deeply coupled convolution–transformer with spatial–temporal complementary learning for video-based person re-identification. *IEEE Transactions on Neural Networks and Learning Systems*.

Liu, X.; Zhang, P.; Yu, C.; Lu, H.; and Yang, X. 2021b. Watching you: Global-guided reciprocal learning for video-based person re-identification. In *Proceedings of the IEEE/CVF conference on computer vision and pattern recognition*, 13334–13343.

McLaughlin, N.; Del Rincon, J. M.; and Miller, P. 2016. Recurrent convolutional network for video-based person re-identification. In *Proceedings of the IEEE conference on computer vision and pattern recognition*, 1325–1334.

Ning, E.; Wang, C.; Zhang, H.; Ning, X.; and Tiwari, P. 2024. Occluded person re-identification with deep learning: A survey and perspectives. *Expert Systems with Applications*, 239: 122419.

Pathak, P.; Eshratifar, A. E.; and Gormish, M. 2020. Video person re-id: Fantastic techniques and where to find them (student abstract). In *Proceedings of the AAAI Conference on Artificial Intelligence*, volume 34, 13893–13894.

Ren, X.; Zhang, D.; Bao, X.; and Zhang, Y. 2022. S²-Net: Semantic and Saliency Attention Network for Person Re-Identification. *IEEE Transactions on Multimedia*, 25: 4387–4399.

Somers, V.; Alahi, A.; and Vleeschouwer, C. D. 2024. Key-point promptable re-identification. In *European Conference on Computer Vision*, 216–233. Springer.

Szegedy, C.; Vanhoucke, V.; Ioffe, S.; Shlens, J.; and Wojna, Z. 2016. Rethinking the inception architecture for computer vision. In *Proceedings of the IEEE conference on computer vision and pattern recognition*, 2818–2826.

Tang, Z.; Zhang, R.; Peng, Z.; Chen, J.; and Lin, L. 2022. Multi-stage spatio-temporal aggregation transformer for video person re-identification. *IEEE Transactions on Multimedia*, 25: 7917–7929.

Wang, T.; Gong, S.; Zhu, X.; and Wang, S. 2014. Person re-identification by video ranking. In *Computer Vision–ECCV 2014: 13th European Conference, Zurich, Switzerland, September 6–12, 2014, Proceedings, Part IV 13*, 688–703. Springer.

Wang, T.; Liu, H.; Song, P.; Guo, T.; and Shi, W. 2022. Pose-guided feature disentangling for occluded person re-identification based on transformer. In *Proceedings of the AAAI conference on artificial intelligence*, volume 36, 2540–2549.

Wang, Y.; Zhang, P.; Gao, S.; Geng, X.; Lu, H.; and Wang, D. 2021. Pyramid spatial-temporal aggregation for video-based person re-identification. In *Proceedings of the IEEE/CVF international conference on computer vision*, 12026–12035.

Wei, Z.; Yang, X.; Wang, N.; and Gao, X. 2021. Flexible body partition-based adversarial learning for visible infrared person re-identification. *IEEE Transactions on Neural Networks and Learning Systems*, 33(9): 4676–4687.

Wen, Y.; Zhang, K.; Li, Z.; and Qiao, Y. 2016. A discriminative feature learning approach for deep face recognition. In *Computer vision–ECCV 2016: 14th European conference, amsterdam, the netherlands, October 11–14, 2016, proceedings, part VII 14*, 499–515. Springer.

Wu, D.; Ye, M.; Lin, G.; Gao, X.; and Shen, J. 2021. Person re-identification by context-aware part attention and multi-head collaborative learning. *IEEE transactions on information forensics and security*, 17: 115–126.

Wu, P.; Wang, L.; Zhou, S.; Hua, G.; and Sun, C. 2024. Temporal correlation vision transformer for video person re-identification. In *Proceedings of the AAAI Conference on Artificial Intelligence*, volume 38, 6083–6091.

Xia, J.; Tan, L.; Dai, P.; Zhao, M.; Wu, Y.; and Cao, L. 2024. Attention disturbance and dual-path constraint network for occluded person re-identification. In *Proceedings of the AAAI Conference on Artificial Intelligence*, volume 38, 6198–6206.

Xiao, Z.; Zhang, Z.; Ning, Y.; Lu, Y.; Song, W.; Qing, X.; and Chen, J. 2024. Deep learning in person re-identification: a survey. In *International Conference on Image Processing and Artificial Intelligence (ICIPAL 2024)*, volume 13213, 939–948. SPIE.

Yan, Y.; Qin, J.; Chen, J.; Liu, L.; Zhu, F.; Tai, Y.; and Shao, L. 2020. Learning multi-granular hypergraphs for video-based person re-identification. In *Proceedings of the IEEE/CVF conference on computer vision and pattern recognition*, 2899–2908.

Yang, J.; Zheng, W.-S.; Yang, Q.; Chen, Y.-C.; and Tian, Q. 2020. Spatial-temporal graph convolutional network for video-based person re-identification. In *Proceedings of the IEEE/CVF conference on computer vision and pattern recognition*, 3289–3299.

Yang, X.; Wang, X.; Liu, L.; Wang, N.; and Gao, X. 2024. STFE: a comprehensive video-based person re-identification network based on spatio-temporal feature enhancement. *IEEE Transactions on Multimedia*, 26: 7237–7249.

Yu, C.; Liu, X.; Wang, Y.; Zhang, P.; and Lu, H. 2024. TF-CLIP: Learning text-free CLIP for video-based person re-identification. In *Proceedings of the AAAI conference on artificial intelligence*, volume 38, 6764–6772.

Yu, C.; Liu, X.; Zhu, J.; Wang, Y.; Zhang, P.; and Lu, H. 2025. CLIMB-ReID: A Hybrid CLIP-Mamba Framework for Person Re-Identification. In *Proceedings of the AAAI Conference on Artificial Intelligence*, volume 39, 9589–9597.

Zang, X.; Li, G.; and Gao, W. 2022. Multidirection and multiscale pyramid in transformer for video-based pedestrian retrieval. *IEEE Transactions on Industrial Informatics*, 18(12): 8776–8785.

Zhang, S.; Luo, W.; Cheng, D.; Yang, Q.; Ran, L.; Xing, Y.; and Zhang, Y. 2024. Cross-platform video person reid: A new benchmark dataset and adaptation approach. In *European Conference on Computer Vision*, 270–287. Springer.

Zhang, T.; Wei, L.; Xie, L.; Zhuang, Z.; Zhang, Y.; Li, B.; and Tian, Q. 2021. Spatiotemporal transformer for video-based person re-identification. *arXiv preprint arXiv:2103.16469*.

Zhang, X.; Zhou, X.; Lin, M.; and Sun, J. 2018. Shufflenet: An extremely efficient convolutional neural network for mobile devices. In *Proceedings of the IEEE conference on computer vision and pattern recognition*, 6848–6856.

Zhang, Z.; He, D.; Liu, S.; Xiao, B.; and Durrani, T. S. 2023. Completed part transformer for person re-identification. *IEEE Transactions on Multimedia*, 26: 2303–2313.

Zhang, Z.; Lan, C.; Zeng, W.; and Chen, Z. 2020. Multi-granularity reference-aided attentive feature aggregation for video-based person re-identification. In *Proceedings of the IEEE/CVF conference on computer vision and pattern recognition*, 10407–10416.

Zhao, Y.; Shen, X.; Jin, Z.; Lu, H.; and Hua, X.-s. 2019. Attribute-driven feature disentangling and temporal aggregation for video person re-identification. In *Proceedings of the IEEE/CVF conference on computer vision and pattern recognition*, 4913–4922.

Zheng, L.; Bie, Z.; Sun, Y.; Wang, J.; Su, C.; Wang, S.; and Tian, Q. 2016. Mars: A video benchmark for large-scale person re-identification. In *Computer Vision–ECCV 2016: 14th European Conference, Amsterdam, The Netherlands, October 11–14, 2016, Proceedings, Part VI* 14, 868–884. Springer.

Zhou, Q.; Zhong, B.; Lan, X.; Sun, G.; Zhang, Y.; Zhang, B.; and Ji, R. 2020. Fine-grained spatial alignment model for person re-identification with focal triplet loss. *IEEE Transactions on Image Processing*, 29: 7578–7589.

Zhou, Z.; Huang, Y.; Wang, W.; Wang, L.; and Tan, T. 2017. See the forest for the trees: Joint spatial and temporal recurrent neural networks for video-based person re-identification. In *Proceedings of the IEEE conference on computer vision and pattern recognition*, 4747–4756.

Zhu, K.; Guo, H.; Liu, S.; Wang, J.; and Tang, M. 2022. Learning semantics-consistent stripes with self-refinement for person re-identification. *IEEE transactions on neural networks and learning systems*.

Zhu, L.; Chen, T.; Ji, D.; Ye, J.; and Liu, J. 2025. Not Every Patch is Needed: Towards a More Efficient and Effective Backbone for Video-based Person Re-identification. *IEEE Transactions on Image Processing*.